AGU100 ADVANCING EARTH AND SPACE SCIENCE

Water Resources Research

RESEARCH ARTICLE
10.1029/2018WR022964

Wildfire Smoke Cools Summer River and Stream Water Temperatures

Aaron T. David[1], **J. Eli Asarian**[2], **and Frank K. Lake**[3]

[1]U.S. Fish and Wildlife Service, Arcata, CA, USA, [2]Riverbend Sciences, Eureka, CA, USA, [3]U.S. Forest Service, Pacific Southwest Research Station, Orleans Ranger Station, Orleans, CA, USA

Key Points:
- Wildfire smoke cools river and stream water temperatures by reducing solar radiation and cooling air temperatures
- For both air and water, smoke has a greater cooling effect on daily maximum temperatures than daily mean temperatures
- This smoke-induced cooling has the potential to benefit cold-water adapted species in fire-prone watersheds

Supporting Information:
- Supporting Information S1

Correspondence to:
A. T. David,
aarontdavid@yahoo.com

Citation:
David, A. T., Asarian, J. E., & Lake, F. K. (2018). Wildfire smoke cools summer river and stream water temperatures. *Water Resources Research*, *54*, 7273–7290. https://doi.org/10.1029/2018WR022964

Received 18 MAR 2018
Accepted 23 AUG 2018
Accepted article online 31 AUG 2018
Published online 4 OCT 2018

Abstract To test the hypothesis that wildfire smoke can cool summer river and stream water temperatures by attenuating solar radiation and air temperature, we analyzed data on summer wildfire smoke, solar radiation, air temperatures, precipitation, river discharge, and water temperatures in the lower Klamath River Basin in Northern California. Previous studies have focused on the effect of combustion heat on water temperatures during fires and the effect of riparian vegetation losses on postfire water temperatures, but we know of no studies of the effects of wildfire smoke on river or stream water temperatures. Wildfire smoke is difficult to quantify, but we successfully used a newly available daily high-resolution (1 km) data set of aerosol optical thickness (AOT) derived from satellite imagery to represent smoke density during 6 years with extensive wildfire activity (2006, 2008, and 2012–2015). Smoke reduced solar radiation by 121 W m^{-2} per 1.0 AOT relative to clear-sky conditions. Linear mixed-effects models showed that on average, smoke cooled daily maximum and mean air temperatures by 0.98 °C and 0.47 °C per 1.0 AOT, respectively, across 19 remote automated weather stations. Smoke had a cooling effect on water temperatures at all 12 river and stream locations analyzed. On average, smoke cooled daily maximum and mean water temperatures by 1.32 °C and 0.74 °C per 1.0 AOT, respectively. This smoke-induced cooling has the potential to benefit cold-water adapted species, particularly because wildfires are more likely to occur during the warmest and driest years and seasons.

1. Introduction

Water temperature is a fundamental regulator of river ecosystems (Beitinger & Fitzpatrick, 1979; Beschta et al., 1987). Temperature influences ecosystem metabolism (Yvon-Durocher et al., 2012), growth rates (Armstrong et al., 2010), reproduction (Ward & Stanford, 1982), and species distributions (Shuter & Post, 1990). For example, the freshwater distributions of Pacific salmon and trout (*Oncorhynchus* spp.) are often constrained by high summer water temperatures (Dunham et al., 2001; Keleher & Rahel, 1996; McCullough, 1999). Indeed, human-induced increases in lotic (stream and river) water temperatures (Caissie, 2006; Poole & Berman, 2001; Webb et al., 2008) have contributed to declines of salmon and trout populations (McCullough, 1999; NAS (National Academy of Sciences), 1996). To guide the restoration of natural thermal regimes in rivers and streams for the benefit of salmonids and other cold-water adapted species, we need to understand the factors that create spatial and temporal thermal variation across the landscape. One phenomenon that can drive variation in lotic water temperatures is wildfire (Gresswell, 1999).

Here we evaluated whether wildfire smoke can reduce lotic water temperatures during the season of peak air and water temperatures within a climatically Mediterranean watershed. While wildfire is a distinctly terrestrial phenomenon, fires can substantially influence aquatic ecosystems (Gresswell, 1999; Minshall et al., 1989; Rieman et al., 2012). Studies of wildfire effects on lotic water temperatures have focused on the effect of the heat of combustion on water temperatures during a fire and the effect of riparian vegetation losses on postfire water temperatures (Beakes et al., 2014; Dunham et al., 2007; Hitt, 2003; Isaak et al., 2010; Mahlum et al., 2011). Water temperatures can rise as a result of direct heating from a fire (Beakes et al., 2014; Gresswell, 1999; Hitt, 2003), although such increases are not ubiquitous and are often short-lived (Beakes et al., 2014; Hitt, 2003; Mahlum et al., 2011). More prolonged impacts have been documented following wildfires on summer water temperatures, which can increase as a result of reduced riparian shading and changes to channel morphology, sometimes for over a decade (Beakes et al., 2014; Dunham et al., 2007; Isaak et al., 2010; Mahlum et al., 2011).

In contrast, to our knowledge, there are no published studies of the effects of wildfire smoke on the water temperatures of streams and rivers, potentially due to the unpredictable nature of wildfires and the challenges of sampling during wildfires. However, indirect evidence suggests that wildfire smoke has the potential to cool river water temperatures. Wildfire smoke particles scatter and absorb incoming solar radiation (Robock, 1988, 1991; Stone et al., 2011), reducing the amount of solar radiation that reaches the Earth's surface (Yu et al., 2016; Zhang et al., 2016), and can consequently reduce air temperatures (Robock, 1988, 1991; Stone et al., 2011; Zhang et al., 2016). Solar radiation and air temperature are important drivers of stream and river water temperatures (Beschta et al., 1987; Caissie, 2006; Johnson, 2004); therefore, wildfire smoke may have the capacity to cool lotic water temperatures. Additionally, Mahlum et al. (2011) and Minshall et al. (1989) speculated that wildfire smoke could shade and cool rivers and streams. Thus, we propose that wildfire smoke can reduce lotic water temperatures via scattering and absorption of solar radiation and associated reductions in air temperature.

Here we examined whether wildfire smoke can cool lotic water temperatures and evaluated the magnitude of the effect of smoke on water temperatures relative to other variables known to influence lotic water temperatures. We also evaluated the effect of wildfire smoke on surface solar radiation and air temperatures. To address these goals we assembled multiyear data on water temperatures, wildfire smoke, solar radiation, air temperatures, precipitation, and river discharge from a large watershed in Northern California. If wildfire smoke does reduce lotic water temperatures, this phenomenon may suggest that historical presuppression fire regimes with greater fire activity may have attenuated maximum summer water temperatures in some watersheds, potentially benefiting salmonids and other cold-water adapted species.

2. Study Area

We conducted our analysis in the lower Klamath River Basin, California, USA (Figure 1). The Klamath River Basin is the third largest watershed draining to the Pacific Ocean in the coterminous USA at ~41,000 km^2. The Klamath River originates in the Cascade Mountains of Southern Oregon and Northern California and then flows into the upper Klamath River Basin, a low relief plateau that historically contained extensive shallow lakes and wetlands (NAS, 2004; VanderKooi et al., 2011). The river then cuts through the southern end of the Cascade Mountains, where it is impounded by a series of five dams. These dams mark the transition from upper to lower basin and divide the watershed by preventing fish passage and altering transport of water and sediment. Below the dams, the Klamath River enters the Klamath-Siskiyou Mountains. In contrast to the upper basin, the lower basin is high relief and the Klamath River and its tributaries primarily flow through confined canyons (NAS, 2004; VanderKooi et al., 2011). Overall the watershed has a Mediterranean climate with warm, dry summers and cool, wet winters (Skinner et al., 2006). However, the climate changes dramatically from interior to coastal and also at finer scales according to elevation, topography, and aspect. The upper basin is generally semiarid and river flows are primarily driven by snowmelt and groundwater, while the lower basin is more mesic and river flows are primary driven by rainfall and snowmelt (NAS, 2004; Williams & Curry, 2011). Conifer and mixed conifer-hardwood forests are the primary vegetation types in the lower Klamath River Basin (Skinner et al., 2006).

We focused our analysis on the lower Klamath River Basin for three reasons. First, the forests of the Klamath-Siskiyou Mountains are fire-prone ecosystems that experience fires of a variety of sizes, intensities, and frequencies (Skinner et al., 2006; Taylor & Skinner, 1998, 2003). In addition to lightning ignitions, Native Americans traditionally used fire to manage natural resources in the basin (Lake, 2007, 2013). Like many forested ecosystems in the western USA, the Klamath-Siskiyou Mountains have been altered by fire suppression and logging, generally resulting in less frequent fires (Skinner et al., 2006; Taylor & Skinner, 1998, 2003). Mean fire size and total area burned have increased recently, however, potentially due to climate change and increased fuel loading resulting from fire suppression (Miller et al., 2012). Second, qualitative evidence suggested that river temperatures are reduced in the basin during periods of heavy smoke from summer wildfires, stimulating interest by natural resource agencies, Native American tribes, and others responsible for recovering Pacific salmon populations in the region (e.g., Robinson, 2013; SRRC (Salmon River Restoration Council), 2014). Third, like many watersheds, the Klamath has been substantially impacted by human activities, including mining, logging, fire suppression, road building, livestock grazing, water diversion, wetland conversion, and impoundment (Klamath River Basin Fisheries Task Force (KRBFTF), 1991;

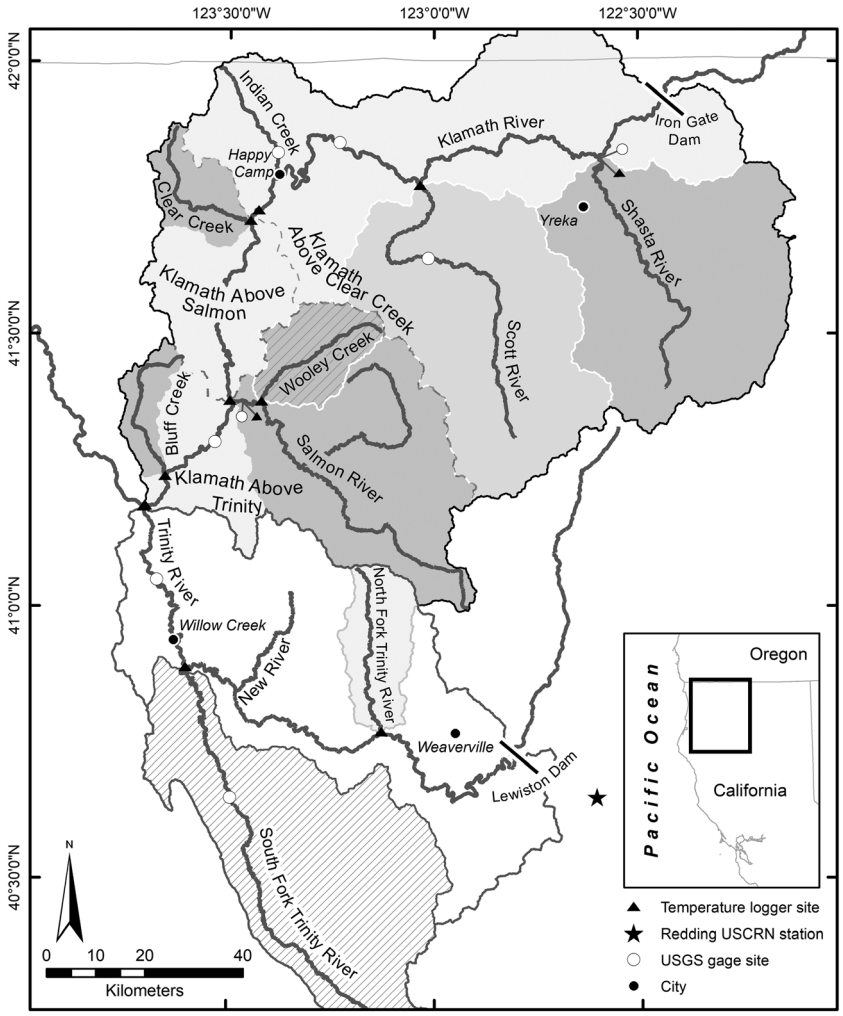

Figure 1. The lower Klamath River Basin with watersheds containing temperature monitoring locations, U.S. Geological Survey gaging stations, and the Redding U.S. Climate Reference Network station indicated.

NAS, 2004). These landscape modifications have resulted in elevated warm-season water temperatures that are a limiting factor for salmon populations in the basin, including spring-run Chinook salmon (*Oncorhynchus tshawytscha*) and Endangered Species Act-listed coho salmon (*Oncorhynchus kisutch*; Bartholow, 2005; KRBFTF, 1991; NAS, 2004; North Coast Regional Water Quality Control Board (NCRWQCB), 2010).

3. Methods

3.1. Water Temperature

An overview of our data sources and analytical methods is found in Figure 2. We confined all data and analyses to 1 June through 30 September of each year because this is the season when water temperatures are typically the highest and most likely to be stressful to cold-water adapted species in the region and when wildfires are most likely to be burning and producing smoke.

We assembled water temperature records from throughout the lower Klamath River Basin that were collected between 1996 and 2015, with the goal of obtaining broad spatial coverage while prioritizing temperature records collected consistently at the same location for multiple years. We identified three temperature records for main stem Klamath River locations and nine for Klamath River tributaries that fit our criteria, each with 15 to 20 years of data (Table 1). These temperature data were collected primarily by the U.S. Forest Service and U.S. Fish and Wildlife Service, supplemented with data collected by the U.S. Bureau of

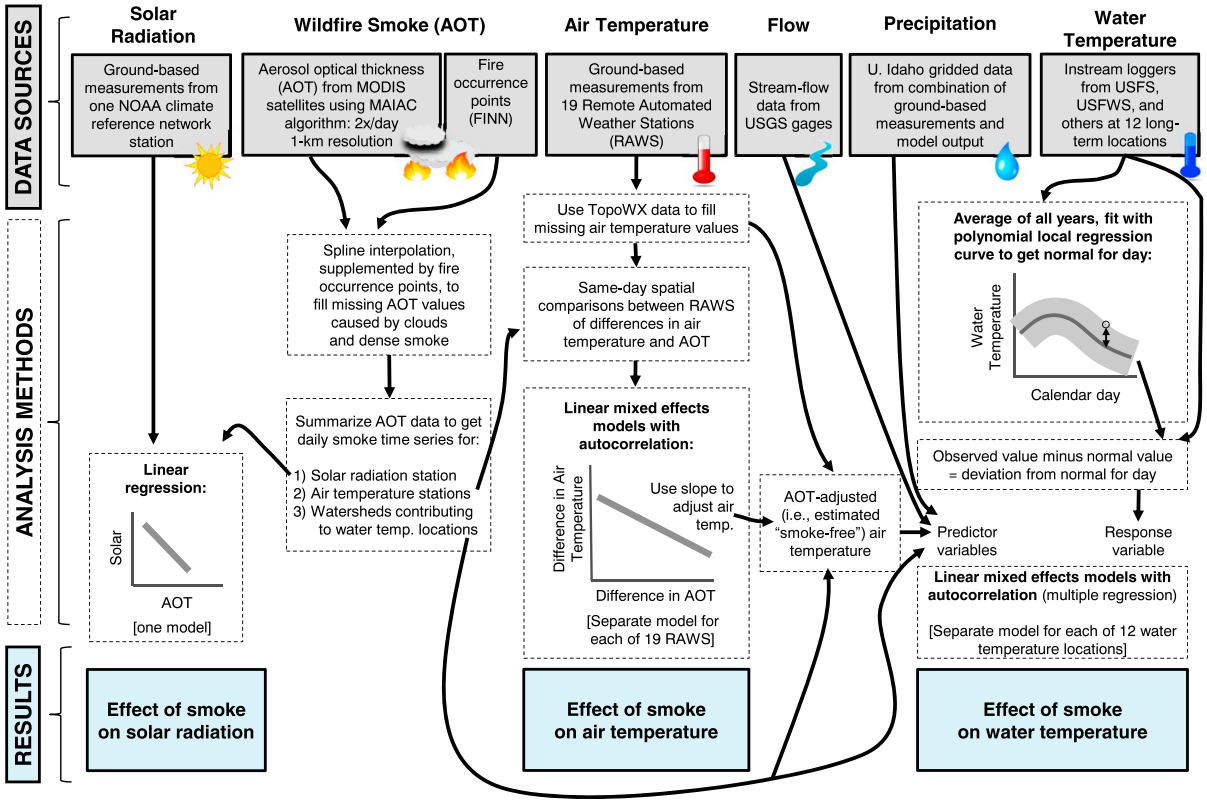

Figure 2. Flow chart and overview of data sources and major data analysis steps used to determine the effects of wildfire smoke on solar radiation, air temperature, and water temperature. For simplicity and clarity, some steps and details are omitted.

Reclamation, Karuk Tribe, and California Department of Water Resources. Water temperatures were measured using digital data loggers and standard protocols (Dunham et al., 2005). Within a year at a location, temperature monitoring did not always encompass the entire 1 June to 30 September period. Because of the multiyear record at these monitoring locations, the type of data logger used and the measurement frequency often changed through time (range: 15–96 min). We calculated daily means, minimums, and maximums from the raw water temperature data. All temperature time series were visually examined and compared with nearby concurrent temperature time series to identify erroneous measurements, which were then removed. Data coverage at individual locations ranged from 81% to 99% (Table 1).

Instead of using the observed temperatures as our response variable in the analyses of wildfire smoke effects on water temperatures, we converted daily mean and maximum water temperatures to deviations from long-term averages on each calendar day. We did this for two reasons. First, we wanted to remove the seasonal pattern water temperatures often exhibit that is not fully captured by variation in air temperature and other meteorological variables (Benyahya et al., 2007; Caissie, 2006). Second, because wildfires and wildfire smoke were not evenly distributed throughout the summer season (see results), we did not want to confound effects of smoke with otherwise normal seasonal variation in water temperatures. For each year at each location, we calculated the long-term average of daily mean and maximum temperatures for each calendar day, excluding data for the current year from the calculation. To smooth out random noise in our long-term averages, we fit a locally weighted second-degree polynomial regression to the daily long-term averages for each year as a function of calendar day. The regression used 20% of the data in fitting each point. We then subtracted the fitted long-term daily average means and maximums from the observed daily means and maximums. The resulting daily mean and maximum water temperature deviations from normal were the values we used for analysis.

3.2. Wildfire Smoke

To determine if wildfire smoke was present over any part of the lower Klamath River Basin for each day between 1 June and 30 September, we examined 250-m resolution, true-color imagery from the Moderate

Table 1
Locations and Characteristics for the 12 Water Temperature Time Series We Analyzed

Location/watershed	Years with data	Number of years	Percent coverage	Data sources	Latitude	Longitude	Drainage area (km^2)	USGS discharge gages
Bluff Cr	1996–2004, 2006–2015	19	81%	FS	41.24054	−123.65453	191.9	Salmon R @ Somes Bar
Clear Cr	1998, 2000–2012, 2014, 2015	16	97%	FS	41.70993	−123.44892	288.5	Indian Cr near Happy Camp
Klamath R above Clear Cr	1996, 1998–2001, 2003–2014	17	95%	FS, FWS	41.72968	−123.42939	7108.3	Klamath R near Seiad Valley + Indian Cr near Happy Camp
Klamath R above Salmon R	1996–2015	20	81%	FS, FWS	41.37908	−123.49777	8138.4	Klamath R @ Orleans -Salmon R @ Somes Bar
Klamath R above Trinity R	1997–2015	19	94%	FS, FWS	41.18607	−123.70179	10790.1	Klamath R @ Orleans
North Fork Trinity R	2001–2015	15	98%	BR, FWS	40.77083	−123.12833	394.2	Salmon R @ Somes Bar
Salmon R	1997–2015	19	85%	FS	41.37639	−123.47706	1944.3	Salmon R @ Somes Bar
Scott R	1998, 2000, 2003–2015	15	93%	FS, KT, BR	41.77509	−123.03471	2107.0	Scott R near Ft. Jones
Shasta R	2000–2015	16	99%	FWS, BR, DWR	41.82415	−122.59449	2055.0	Shasta R near Yreka
South Fork Trinity R	1997–1999, 2001–2015	18	89%	FWS, FS	40.88944	−123.60278	2412.3	South Fork Trinity R below Hyampom
Trinity R	1998–2015	18	92%	FS, FWS	41.18446	−123.70673	5826.2	Trinity R @ Hoopa
Wooley Cr	1998–2001, 2003–2015	17	83%	FS	41.37824	−123.42122	384.9	Salmon R @ Somes Bar

Note. Percent coverage = percentage of days within the years with data that have temperature data; FS = U.S. Forest Service; FWS = U.S. Fish and Wildlife Service; BR = U.S. Bureau of Reclamation; KT = Karuk Tribe; DWR = California Department of Water Resources.

Resolution Imaging Spectroradiometer (MODIS) instruments on board the National Aeronautics and Space Administration's (NASA) Terra and Aqua satellites. This imagery was available starting with 2004 from NASA Worldview (https://worldview.earthdata.nasa.gov/). Terra and Aqua have Sun-synchronous, near-polar orbits. Terra passes over Northern California each morning and Aqua each afternoon. Smoke was typically easy to distinguish in imagery (Figure 3a). To confirm we were not misinterpreting the imagery, we used a spatial database of U.S. wildfires (Short, 2014, 2017) to identify when fires were burning in or near the lower Klamath Basin. The database and our observations in the region both indicated that the MODIS imagery accurately captured the occurrence of wildfire smoke in the lower Klamath Basin and that 2006, 2008, and 2012–2015 were moderately to very smoky summers. Unless otherwise stated, all further analyses use only those years.

We also used MODIS data to quantify the distribution and density of wildfire smoke. The measure of smoke we used was aerosol optical thickness (AOT), the degree to which aerosols prevent the transmission of light through the atmosphere by absorption or scattering. AOT is a unitless number that ranges from near 0 (completely clear skies with no dust, haze, or smoke) to 4 (exceptionally smoky or hazy conditions). We used 1-km resolution gridded AOT data derived from multiple MODIS spectral bands processed according to the multiangle implementation of atmospheric correction algorithm (MAIAC; Di et al., 2016; Lyapustin, Martonchik et al., 2011; Lyapustin, Wang et al., 2011; Lyapustin, Korkin et al., 2012; Lyapustin, Wang, Laszlo, Hilker et al., 2012; Lyapustin, Wang, Laszlo, Korkin, 2012), downloaded from the NASA Center for Climate Simulations FTP portal (ftp://maiac@dataportal.nccs.nasa.gov/DataRelease). These AOT data were available from 1 to 3 times per day, depending on the location of satellite passes. While the MAIAC algorithm improves upon other AOT retrieval methods, it is often unable to retrieve AOT from grid cells where clouds or dense smoke are present (Figure 3b; Lyapustin, Martonchik et al., 2011; Lyapustin, Wang et al., 2011; Lyapustin, Korkin et al., 2012; Lyapustin, Wang, Laszlo, Korkin, 2012; Superczynski et al., 2017). These null values are nonrandom and thus need to be infilled to avoid bias. We used the Fire INventory from NCAR (FINN; Wiedinmyer et al., 2011) fire occurrence data set along with a spatial interpolation algorithm to infill the null values. FINN is a spatially explicit fire occurrence data set derived from MODIS thermal anomaly data with a 1-km spatial resolution and a daily temporal resolution (Wiedinmyer et al., 2011). If an AOT grid cell with a null value contained a FINN fire occurrence for the same day, we assigned that grid cell an AOT of 3.0 (75% of the maximum possible value of 4.0, selected based on visual exploration). After

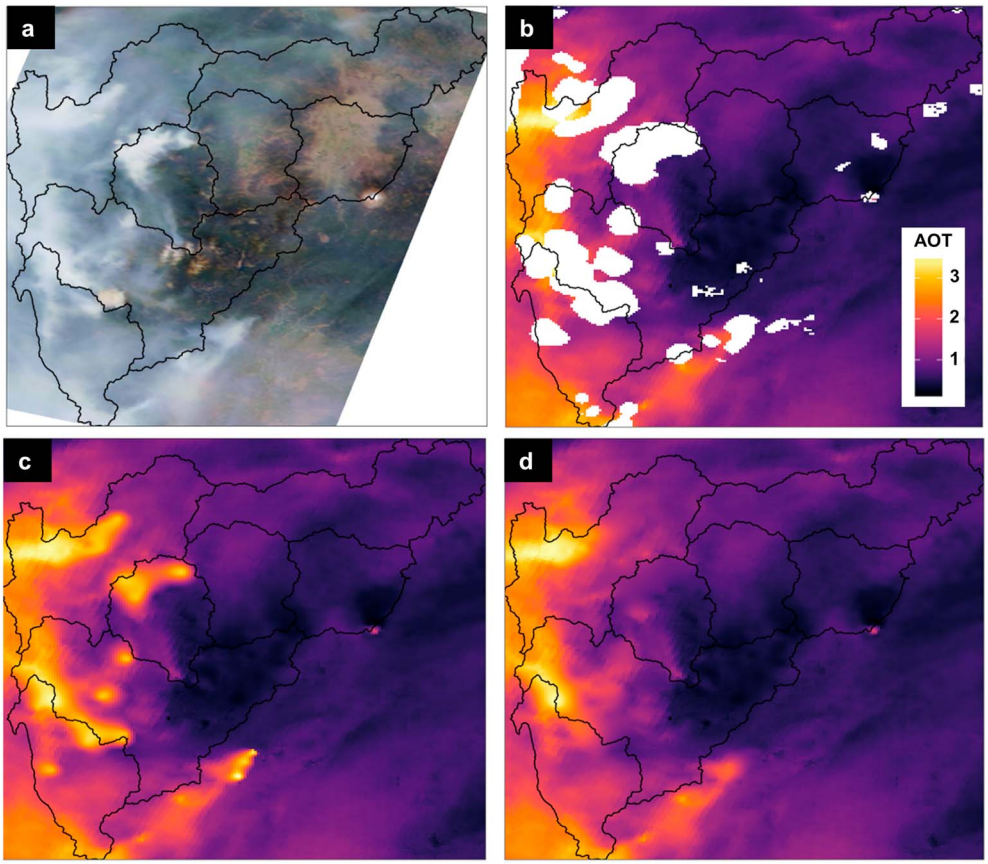

Figure 3. (a) Visible Moderate Resolution Imaging Spectroradiometer imagery for an example satellite pass (Terra on 12 July 2008); (b) original multiangle implementation of atmospheric correction algorithm-derived aerosol optical thickness (AOT) before interpolation of null values due to clouds or dense smoke; (c) AOT with Fire INventory from NCAR (FINN) points inserted and then interpolated; (d) AOT interpolated to fill null values without FINN points. The black lines are boundaries of subbasins (level 4 hydrologic units) in the Klamath River Basin.

assigning the FINN fire occurrences, we used the Close Gaps with spline function (Conrad, 2010) from the System for Automated Geoscientific Analyses (Conrad et al., 2015), implemented within the R software for statistical computing (R Core Team, 2015) using the rsaga package's (Brenning, 2008) rsaga.geoprocessor function, to spatially interpolate the remaining null-value grid cells in each satellite pass. The Close Gaps with spline function uses observed values where present and fills in gaps by fitting spline functions to the observed data (Mitášová & Mitáš, 1993). Advantages of this method include allowing interpolated values to be greater than input values, which is necessary given that some null values were due to dense smoke whereas nearby areas of lighter smoke were not null (Reid et al., 2015). After interpolation, all values greater than 4.0 (the maximum possible AOT value) were reduced to 4.0. We also ran the same interpolation algorithm for each satellite pass without the FINN data for comparison. The results were two sets of fully infilled gridded AOT data for each MODIS pass over Northern California (FINN-interpolated, Figure 3c; and no-FINN interpolated, Figure 3d). To choose which gridded AOT data from each satellite pass to use in analyses, we visually examined the original AOT data with null values, the FINN-interpolated AOT data, the no-FINN interpolated AOT data, and the corresponding MODIS true color image. We discarded all satellite passes when the AOT data did not fully encompass our study area (239 of 1,748 passes). For most passes we chose the FINN-interpolated version but substituted no-FINN interpolations when the FINN interpolations performed poorly (100 of 1,509 passes), typically due to a combination of smoke and cloud cover. Finally, we discarded two passes for which neither the FINN nor the no-FINN interpolations produced gridded AOT data that reasonably matched the associated true-color MODIS image. Across all satellite passes selected for analysis on days when wildfire smoke was present over the lower Klamath

Basin, the mean proportion of infilled grid cells was 19.8% for the watersheds upstream of the temperature monitoring locations.

Once we finalized our sets of AOT data for analysis, we calculated mean AOT values for the watersheds upstream of the 12 water temperature monitoring locations during each day within our period of interest. For the main stem Klamath and Trinity river monitoring locations we truncated their upstream watersheds at the lower most dams because the thermal inertia of the upstream reservoirs and the long distance between the dams and monitoring locations should make temperatures at these locations relatively insensitive to smoke upstream of the dams. If there were more than a single pass for each satellite in a day, we first calculated the mean AOT value of each satellite within that day, and then calculated the mean AOT value of the two satellites for each day. On cloudy, smoke-free days, the interpolation algorithm often appeared to overestimate AOT values. Thus, within each watershed, for all days when we had previously determined there was no smoke present anywhere in the lower Klamath Basin using the MODIS true-color imagery, we assigned those days the lower quartile of all that watershed's daily mean AOT values for smoke-free days. The mean difference between the original daily AOT values and the uniform lower quartile AOT values across the 12 watersheds was 0.11 (range: 0 to 0.90). Because the Klamath Basin is situated along the Pacific Coast in an area of low population density, wildfire smoke is the primary producer of aerosols in the region (e.g., CARB (California Air Resources Board), 2013). Thus, assigning a uniform low AOT value to all smoke-free days should not bias our analysis. Finally, for 11 days that were classified as smoky but did not have at least one valid set of AOT data, we assigned those days the mean of the AOT values from the day before and the day after.

3.3. Solar Radiation, Air Temperature, Precipitation, and River Discharge

We assembled meteorological and river discharge data to assess the influence of smoke density (AOT) on surface solar radiation and air temperature in our study region and to evaluate as drivers of water temperature variation. We used the Redding, California station of the U.S. Climate Reference Network (USCRN; https://www.ncdc.noaa.gov/crn/) to quantify the effect of wildfire smoke on surface solar radiation. Hourly solar radiation data were available starting in 2003. For each day between 1 June and 30 September, we calculated the mean solar radiation (W m^{-2}) between 09:00 and 17:00 LST across 2003–2015. Next, we identified the maximum value of mean solar radiation for each calendar day across this time period. We assumed this maximum value represented completely clear-sky conditions (i.e., no clouds or smoke). For the six focal years, we then calculated the difference between the observed mean solar radiation on each day and the maximum solar radiation value under clear-sky conditions for the same calendar day. Using the process described in the Wildfire Smoke section, we also calculated daily mean AOT values for a 1-km radius circle around the Redding USCRN station for the six focal years.

Air temperatures from 19 remote automated weather stations (RAWS; Table S1 in the supporting information) in the lower Klamath Basin were used to quantify the effect of wildfire smoke on air temperature and for evaluation as a driver of water temperature variation. Daily maximum and minimum air temperatures for each RAWS were downloaded from the Western Regional Climate Center (https://wrcc.dri.edu/) and were averaged to obtain daily means. We examined time series of temperatures at nearby RAWS to identify erroneous observations, which were then removed. Short, within-year gaps due to missing or erroneous observations were filled using quality assured and infilled temperatures at their respective RAWS from the Topography Weather gridded meteorological data set (Oyler et al., 2015). For two RAWS that were not installed until after 2008, we used separate generalized least squares regressions (Zuur et al., 2009) and daily mean temperatures from two neighboring RAWS to predict the missing temperatures. The regressions were implemented using the function gls in the nlme R package (Pinheiro et al., 2017) and included a first-order autoregressive correlation structure nested within years to account for the temporal nature of the data. Predicted temperatures from the two neighboring RAWS were averaged to produce the final temperature estimates. The results were daily mean air temperatures for 1 June through 30 September 2006, 2008, and 2012–2015 for the 19 RAWS. In total, 7.7% of air temperature observations were infilled using either the Topography Weather data set or the regressions. Similarly to the solar radiation data, we used the process described in the Wildfire Smoke section to calculate daily mean AOT values for a 1-km radius circle around each RAWS for the six focal years, except that we applied a uniform lower-quartile AOT value for nonsmoky days across all 19 RAWS.

We assembled daily mean accumulated precipitation for the watersheds upstream of the 12 temperature monitoring locations from the University of Idaho gridded meteorological data set (Abatzoglou, 2013),

processed through the U.S. Geological Survey geo data portal (Blodgett et al., 2011; https://cida.usgs.gov/gdp/). These precipitation data are derived at a 4-km spatial resolution for the coterminous USA using a combination of daily data from the North American Land Data Assimilation System Phase 2 (Mitchell et al., 2004) and monthly data from the Parameter-Elevation Regressions on Independent Slopes Model (Daly et al., 2008). Finally, we compiled daily mean discharges for eight gaging stations on the Klamath River and its tributaries from the U.S. Geological Survey (Table 1; http://waterdata.usgs.gov/nwis).

3.4. Analysis

We used linear regression to evaluate the effect of wildfire smoke (daily mean AOT) on daily differences between observed solar radiation and maximum potential clear-sky solar radiation at the Redding USCRN station. To isolate the effect of smoke, we used only cloud-free days in the regression, as determined by visual examination of MODIS true-color imagery. While these data constitute a time series, we did not incorporate any temporal correlation structure in the regression. In the absence of external forcing (e.g., smoke and clouds), daily solar radiation varies in a predictable manner and there should not be any lagged effects, precluding the need to account for the temporal structure of these data.

We used linear mixed-effects models (Zuur et al., 2009) to evaluate the effect of wildfire smoke on daily mean and maximum air temperatures. The models were implemented using the function lme in the nlme R package (Pinheiro et al., 2017). We calculated differences between daily air temperatures and AOT values at each RAWS and all other RAWS across the six focal years, except for the two RAWS installed after 2008, for which we calculated differences only for 2012–2015. We used air temperature differences instead of raw air temperatures to partition out the influence of natural drivers of air temperature such as cloud cover, atmospheric pressure, and day length that vary day-to-day, but that should be relatively homogeneous across the lower Klamath Basin within a day. For each RAWS, we fit separate models of daily mean and maximum air temperature differences as a function of AOT differences. Each model included nested random intercepts of RAWS and year within RAWS to account for natural air temperature differences due to elevation, distance from the coast, and other aspects of geography, along with potential variation in these differences among years. Within each RAWS by year combination we incorporated a first-order autoregressive correlation structure to account for the temporal nature of the data.

Because we were concerned that including air temperatures affected by wildfire smoke as an explanatory variable in our water temperature models would result in biased estimates of the effect of smoke, we next calculated estimates of smoke-free air temperatures. We adjusted air temperatures upward at each RAWS by multiplying the AOT coefficient from the mean air temperature difference model for a RAWS with the observed AOT values at that RAWS and then added the resulting values to the daily mean air temperatures at that RAWS. For the two RAWS installed after 2008, we used the infill regressions developed earlier with the AOT-adjusted air temperatures at the two neighboring RAWS to estimate the 2006 and 2008 AOT-adjusted air temperatures. For each of the 12 water temperature monitoring locations, we then calculated average daily air temperatures using all relevant RAWS (Table S1, almost exclusively those RAWS within the watershed upstream of the monitoring location), both for AOT-adjusted and unadjusted air temperatures.

We also used linear mixed-effects models to evaluate the effect of wildfire smoke and other variables on daily mean and maximum water temperature deviations. A random intercept of year was included in the models because water temperatures can vary overall year to year. Within each year we incorporated a first-order autoregressive correlation structure to account for the temporal nature of the data and the thermal inertia of water. For each of the 12 water temperature monitoring locations and two response variables, we fit 15 separate models that represented all possible combinations of the explanatory variables wildfire smoke (AOT), adjusted air temperature, precipitation, and river discharge. Specifically, we used 3-day trailing averages of AOT, air temperature, and precipitation, and daily values of river discharge. We ranked model performance using Akaike's information criterion (AIC), a relative measure of model fit to the data, with a penalty for increasing model complexity. The model with the lowest AIC value is considered the best performing model of those evaluated. If two models had identical AIC values, we chose the simpler model as the best-performing. We then refit the best-performing models with unadjusted air temperatures to assess changes in the effect of AOT. To evaluate the robustness of our results to two of

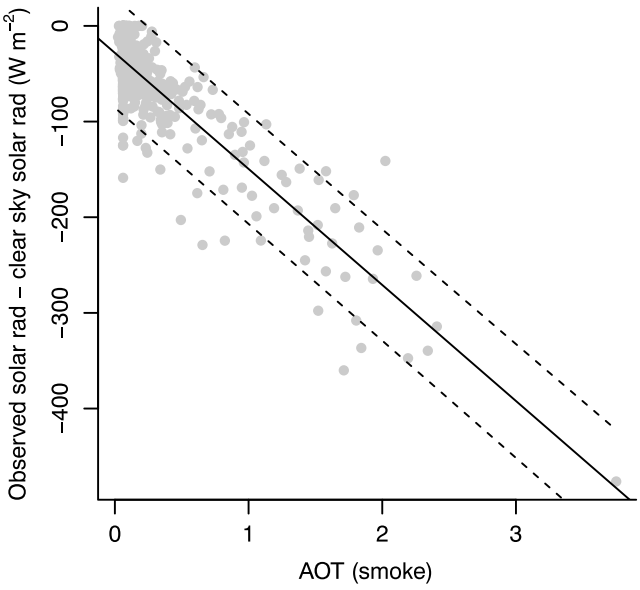

Figure 4. Differences between observed and clear-sky potential daily mean solar radiation at the U.S. Climate Reference Network station near Redding, California on cloud-free days between 1 June and 30 September 2006, 2008, and 2012–2015 as a function of remotely sensed wildfire smoke (daily mean aerosol optical thickness). The solid line is the regression line, and the dotted lines are 95% confidence intervals for the prediction of new values.

our major methodological decisions (using a uniform AOT value on nonsmoky days and using water temperature deviations from normal as the response variable rather than observed water temperatures), we also fit two alternate formulations of the water temperature models (Text S1 in the supporting information).

As a simple alternative measure of the effect of smoke on water temperatures, we calculated the average differences in daily mean and maximum water temperature deviations between nonsmoky (3-day average AOT < 0.1) and at least moderately smoky (3-day average AOT ≥ 0.5) days at each water temperature monitoring location within each year. Differences were only calculated when there were at least 5 days within each category.

4. Results

4.1. Solar Radiation

Wildfire smoke had a strong negative effect on solar radiation at the Redding USCRN station ($F_{1,550} = 1703$, $P < 0.001$, $\beta = -121$ W m^{-2} per 1.0 AOT; Figure 4), explaining 76% of the variation in daily differences between observed and clear-sky potential radiation on cloud-free days. This represents an approximately 14% decrease in daily mean solar radiation per 1.0 AOT. On the single smokiest day (3.75 AOT), solar radiation was reduced by more than 450 W m^{-2} relative to clear-sky potential, while on other moderate and heavy smoke days (i.e., AOT ≥ 0.5) solar radiation was often reduced between 50 and 350 W m^{-2} relative to clear-sky potential.

4.2. Air Temperature

Wildfire smoke had a cooling effect on both daily mean and maximum air temperatures at all 19 lower Klamath Basin RAWS (Table S1 and Figures S1 and S2 in the supporting information). The effect was stronger for maximum than mean temperatures, with an average expected reduction in maximum air temperature of 0.98 °C per 1.0 AOT and an average expected reduction in mean air temperature of 0.47 °C per 1.0 AOT across the 19 RAWS. Expected reductions in maximum air temperatures ranged from 0.40 °C to 1.47 °C per 1.0 AOT, while expected reductions in mean air temperatures ranged from 0.14 °C to 0.75 °C per 1.0 AOT (Table S1).

4.3. Water Temperature

During the six focal years, significant wildfire smoke production generally began in late July and continued through early to mid-September, with the exception of 2008, when widespread fires throughout California produced extensive smoke beginning in late June (Figure S3). Maximum observed values of 3-day averaged AOT varied among the watersheds upstream of the 12 temperature monitoring locations, from 1.255 for the Klamath River above Clear Creek to 2.661 for Bluff Creek (Table 2). The best-performing models of both daily mean and maximum water temperature deviations included wildfire smoke for all 12 monitoring locations (Tables 2, S2, and S3). Wildfire smoke had a cooling effect on water temperatures in all the best-performing models, with the second largest effect size after air temperature in all 12 maximum temperature models and 10 of 12 mean temperature models (Table 2 and Figure 5). The average expected reduction in daily maximum water temperature deviations was 1.32 °C per 1.0 AOT across the 12 monitoring locations. Expected reductions in maximum water temperatures ranged from 0.56 °C per 1.0 AOT for Wooley Creek to 2.73 °C per 1.0 AOT for the Shasta River (Table 2). The average expected reduction in daily mean water temperature deviations was 0.74 °C per 1.0 AOT across the 12 monitoring locations. Expected reductions in mean water temperatures ranged from 0.28 °C for Wooley Creek to 1.23 °C for the Shasta River (Table 2). When we refit the best-performing models using air temperatures unadjusted for AOT, the estimated effects of wildfire smoke on water temperatures were generally 0.1 to 0.2 °C per 1.0 AOT smaller than in the models with adjusted air temperatures (Table 2). Discharge was included in five of the best-performing models of maximum temperatures and seven of the best-performing models of mean temperatures. Precipitation was included in eight of the best-performing models of maximum temperatures and six of the best-performing models of mean

Table 2
Best-Performing Models of Daily Maximum and Mean Water Temperature Deviations for the 12 Water Temperature Monitoring Locations in the Lower Klamath River Basin

		Daily maximum water temperatures				Daily mean water temperatures			
Location/ watershed	Max AOT	Best-performing model	ΔT_W per 1.0 AOT (°C)	SE (°C)	Unadjusted T_A ΔT_W per 1.0 AOT (°C)	Best-performing model	ΔT_W per 1.0 AOT (°C)	SE (°C)	Unadjusted T_A ΔT_W per 1.0 AOT (°C)
Bluff Cr	2.661	$T_A - AOT$	1.29	0.13	1.23	$T_A - AOT - Q + P$	0.61	0.08	0.56
Clear Cr	2.036	$T_A - AOT$	0.86	0.13	0.78	$T_A - AOT - Q$	0.38	0.09	0.30
Klamath R above Clear Cr	1.255	$T_A - AOT - P$	1.83	0.25	1.67	$T_A - AOT - P$	1.14	0.19	0.98
Klamath R above Salmon R	1.285	$T_A - AOT - Q - P$	0.82	0.17	0.69	$T_A - Q - AOT$	0.55	0.14	0.42
Klamath R above Trinity R	1.370	$T_A - AOT - Q$	0.85	0.16	0.74	$T_A - AOT - Q$	0.67	0.13	0.56
North Fork Trinity R	2.396	$T_A - AOT - P$	1.07	0.15	0.93	$T_A - AOT - P$	0.51	0.10	0.38
Salmon R	1.728	$T_A - AOT - Q - P$	0.93	0.15	0.81	$T_A - AOT - Q$	0.46	0.10	0.34
Scott R	1.394	$T_A - AOT - P$	2.35	0.32	2.23	$T_A - AOT$	1.16	0.18	1.02
Shasta R	1.314	$T_A - AOT - P$	2.73	0.42	2.55	$T_A - AOT - P$	1.23	0.25	1.02
South Fork Trinity R	2.277	$T_A - AOT + Q - P$	1.50	0.19	1.39	$T_A - AOT + Q$	0.93	0.11	0.81
Trinity R	2.321	$T_A - AOT - Q - P$	1.10	0.16	0.98	$T_A - Q - AOT - P$	0.92	0.14	0.81
Wooley Cr	2.458	$T_A - AOT$	0.56	0.11	0.45	$T_A - AOT - P$	0.28	0.10	0.17

Note. Variables in the best-performing model columns are ordered from left to right in terms of decreasing effect size according to variable *t* scores. The sign in front of a variable indicates the direction (positive or negative) of that variable's effect. Max AOT = the highest 3-day averaged AOT observed in the watershed upstream of each temperature monitoring location during the six focal years; ΔT_W per 1.0 AOT = AOT parameter coefficient (expected water temperature reduction); SE = standard error of the AOT parameter coefficient; T_A = air temperature; Q = discharge; P = precipitation. Unadjusted T_A = air temperature unadjusted for the effect of AOT.

temperatures. Both discharge and precipitation had cooling effects on water temperature except discharge in the South Fork Trinity River and precipitation on mean temperatures in Bluff Creek (Table 2). The two alternate formulations of the water temperature models produced similar results (Text S1 and Tables S4, S5, S6, S7, S8, and S9), suggesting that our results were robust to two of our major methodological decisions.

Days that were at least moderately smoky (3-day average AOT ≥ 0.5) were generally cooler relative to normal than smoke-free days (3-day average AOT < 0.1) within years at individual monitoring locations (Figures 6 and 7). Average differences within locations and years ranged from 0.77 °C warmer relative to normal on smoky days for the Trinity River in 2006 to 4.49 °C cooler relative to normal on smoky days for the North Fork Trinity River in 2015.

5. Discussion

5.1. Summary

We used a novel application of a recently developed data set of atmospheric AOT at high spatial and temporal resolutions to evaluate the effect of wildfire smoke on lotic water temperatures and two of the primary drivers of lotic water temperatures: solar radiation and air temperature. While other studies have explored the effects of wildfire smoke on solar radiation and air temperature, to our knowledge, this study is the first to formally test the hypothesis that wildfire smoke can cool river water temperatures. Our results support this hypothesis, indicating that wildfire smoke had a cooling effect on water temperatures at all 12 locations analyzed within the lower Klamath River Basin. We also found that wildfire smoke had a negative effect on solar radiation and a cooling effect on air temperatures. Together, these results suggest that wildfire smoke can be a natural mechanism to reduce summer water temperatures in watersheds where wildfires occur frequently.

5.2. Smoke Effects on Solar Radiation and Air Temperature

Theory and previous analyses have also demonstrated that wildfire smoke can reduce the amount of solar radiation that reaches the Earth's surface through a combination of absorption and scattering of radiation by the aerosols that comprise wildfire smoke (Robock, 1988, 1991; Stone et al., 2011; Yu et al., 2016; Zhang et al., 2016). Precise comparisons of the magnitude of smoke's effect on solar radiation among studies are hampered by methodological differences such as solar zenith angle (i.e., season and time of day) and AOT measurement; nonetheless, our estimate of a 121-W m^{-2} reduction in solar radiation per 1.0 AOT is similar

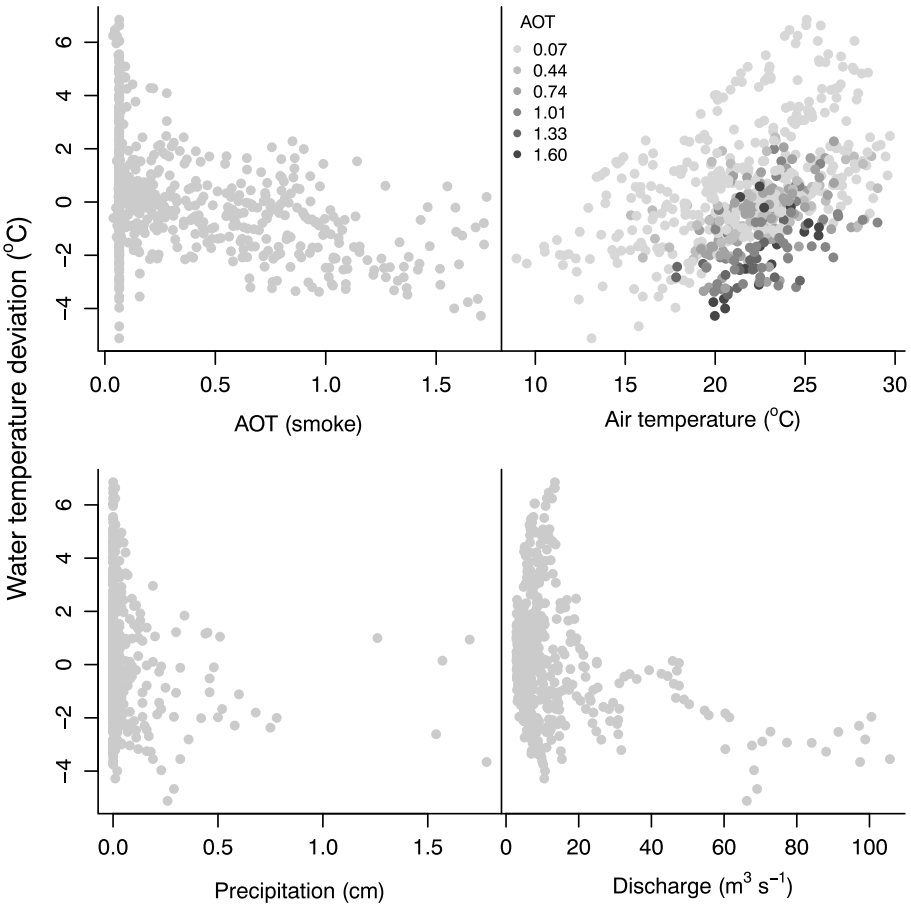

Figure 5. Daily maximum water temperature deviations at an example location (the Salmon River) as a function of remotely sensed wildfire smoke (mean aerosol optical thickness, AOT), AOT-adjusted mean air temperature, mean accumulated precipitation, and mean river discharge. Points in the air temperature panel are shaded according to their corresponding AOT values. AOT, air temperature, and precipitation are 3-day trailing averages, while discharge is a daily value.

to three recent estimates of the effects of wildfire smoke on solar radiation. Measurements across multiple solar zenith angles and two locations during a wildfire in Colorado by Stone et al. (2011) averaged 136 W m^{-2} per 1.0 AOT, resulting in a diurnally integrated estimate of 61.5 W m^{-2} per 1.0 AOT. Our estimate also matched the lower range of estimated reductions of 120 to 140 W m^{-2} per 1.0 AOT around solar noon identified by Yu et al. (2016) for a large wildfire in the California Sierra Nevada Mountains and was almost identical to the estimated reductions at three of four locations in the midwest USA analyzed by Zhang et al. (2016).

The attenuation of solar radition by smoke resulted in cooler air temperatures. Because of different methodologies, it is difficult to compare our results with other studies that evaluted the effects of wildfire smoke on air temperatures. However, most estimates of the cooling effect of smoke in Zhang et al. (2016) ranged from 0.25 °C to 1.0 °C per 1.0 AOT for early afternoon air temperatures, which fall within the range of effects we observed on mean and maximum air temperatures. Our results mirror previous analyses showing that wildfire smoke has a stronger cooling effect on maximum than mean air temperatures. For example, Robock (1988) found that smoke trapped by an inversion in the Klamath River canyon during wildfires in September 1987 resulted in daily maximum air temperatures reduced to 20 °C below normal, while daily minimum air temperaturs were only slightly affected. This difference is likely because smoke strongly affects shortwave (visible) solar radiation during the day, when maximum temperatures usually occur. In contrast, smoke only nominally affects longwave (infrared) radiation, the dominant radiational forcing at night when minimum temperatures usually occur (Robock, 1988, 1991; Stone et al., 2011).

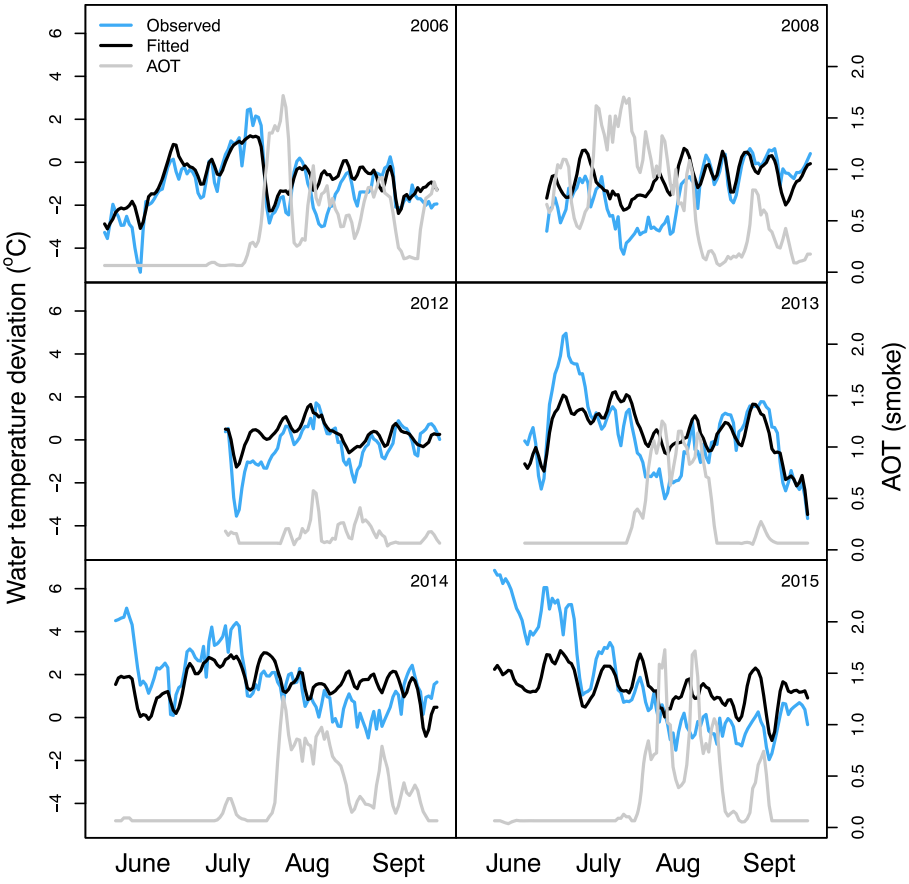

Figure 6. Time series for each year of daily maximum water temperature deviations at an example location (the Salmon River), fitted values from the best-performing model of Salmon River water temperatures, and 3-day averaged mean aerosol optical thickness in the Salmon River watershed.

5.3. Smoke Effects on Water Temperature

The reduction of solar radiation by wildfire smoke and associated reductions in air temperature likely form the physical basis for the cooling effect of smoke on water temperatures we observed. Solar radiation and air temperature are two of the most important determinants of stream and river water temperatures (Beschta et al., 1987; Caissie, 2006; Johnson, 2004). Wildfire smoke had a stronger cooling effect on maximum than mean water temperatures at all 12 monitoring locations, likely for similar reasons as air temperature. Smoke has significant effects on solar radiation and air temperatures during the day when maximum water temperatures usually occur but has little effect at night when minimum water temperatures usually occur.

Notably, there was greater than a fourfold difference between the largest and smallest smoke effects among the monitoring locations for both daily mean and maximum water temperatures. These differences may in part be due to variation in sensitivity to solar radiation among the upstream watersheds. For example, the Shasta and Scott river watersheds, which had the largest smoke effects, both contain large alluvial valleys with minimal topographic shading of the river channels. Additionally, these valleys have been modified extensively for agricultural production, leading to lower streamflow, reduced shading by riparian vegetation, and simplification of the river channels. Together, these factors likely make these rivers more sensitive to daily variation in solar radiation and air temperature. In contrast, Wooley Creek, which had the smallest effect of smoke, is in a steep, confined watershed that is almost entirely forested, reducing the sensitivity of the creek and its tributaries to variation in solar radiation. Wooley Creek is also almost entirely within a wilderness area, with few human impacts that could increase sensitivity to external energy inputs. We suggest future studies on this topic to identify watershed features that influence sensitivity to the effect of smoke. Other features that may be useful to consider include topography, elevation, aspect, and drainage area.

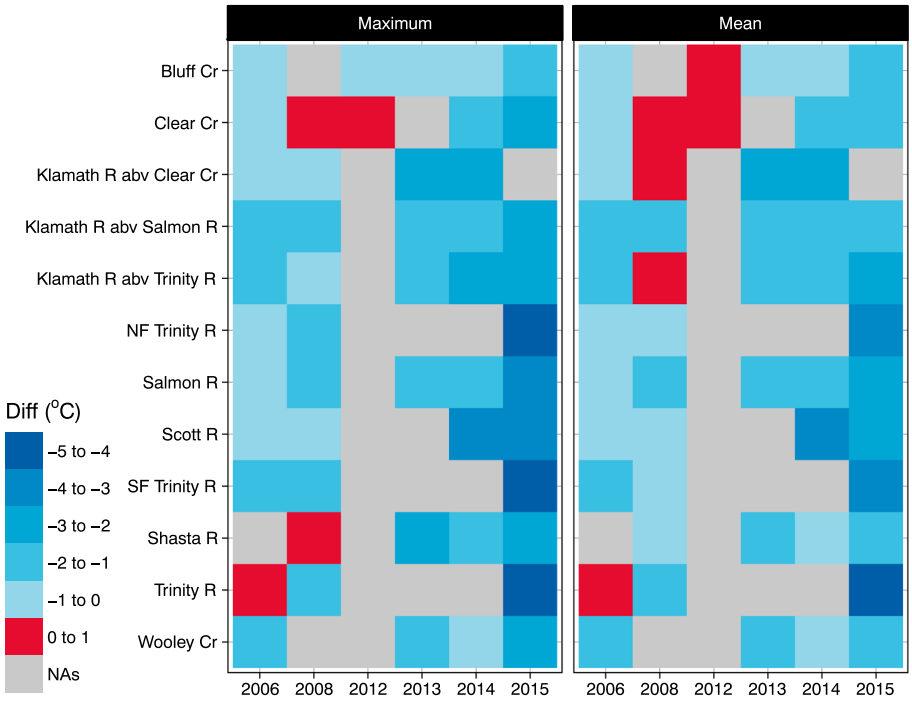

Figure 7. Average differences in daily maximum and mean water temperature deviations between nonsmoky (3-day average aerosol optical thickness [AOT] < 0.1) and at least moderately smoky (3-day average AOT ≥ 0.5) days at each monitoring location within each year. Differences were only calculated when there were at least 5 days within each category. The color gray indicates no data or insufficient days within a category.

When we refit the best-performing models for each monitoring location using air temperatures unadjusted for the effect of smoke, the effect of smoke on water temperatures was diminished at all locations. While the differences were modest (generally 0.1 to 0.2 °C per 1.0 AOT) relative to differences in the effects among monitoring locations, these differences support our expectation that wildfire smoke influences lotic temperatures both directly by modulating solar radiation and indirectly by cooling air temperatures.

5.4. Sources of Uncertainty

While we are confident that both our approach and data were appropriate for testing the hypotheses we posed, there are sources of uncertainty in our analysis that are important to examine for potential future improvement. These include representation of temperature inversions, better methods for filling spatial gaps in AOT, improved quantification of AOT under cloudy and heavy smoke conditions, improved representation of multiday effects of smoke on air and water temperatures, and alternate water temperature modeling frameworks.

Under stable atmopheric conditions, temperature inversions in the incised topography of the lower Klamath River Basin can trap smoke in river canyons (Estes et al., 2017; Robock, 1988; Skinner et al., 2006). This phenomenom can be self-reinforcing because the inversion increases smoke pooling in the river canyons, which strengthens the cooling effect of smoke, further stabalizing the inversion (Estes et al., 2017; Robock, 1988; Skinner et al., 2006). We did not try to quantify the effect of inversions, but this would be a useful topic to explore. For example, a day when smoke is trapped under an inversion in the river canyons may overall only have a modest watershed mean AOT value due to the small area covered by smoke relative to the whole watershed; however, because the smoke is concentrated over the stream network, it may still exert a strong influence on water temperatures. Additionally, because of the inversions, alternate spatial interpolation techniques such as local (i.e., moving window) regression kriging (e.g., Gräler et al., 2016) of AOT that use elevation or topographic position as predictor variables could improve upon the spline interpolation method that we used, which ignores topography.

Multiangle implementation of atmospheric correction algorithm is the best available algorithm for quantifying AOT but may still be improved to perform better during cloudy or extremely smoky conditions. While the MAIAC AOT data in conjunction with our approach to filling null-value grid cells generally appeared to accurately capture the distribution of smoke shown in MODIS imagery, during some satellite passes when there were both clouds and smoke, the infilled AOT data failed to accurately reflect the distribution of smoke in the corresponding true-color image. After we completed our analyses, an updated version of the MAIAC algorithm and AOT data were released (Lyapustin et al., 2018); however, in regard to the above issues, our brief examination of the updated data did not indicate substantial improvement relative to the version we used.

More complex representations of multiday smoke dynamics might also improve our analysis. By only analyzing intraday differences in AOT, we did not account for potential cumulative effects of smoke on air temperatures over longer time periods. In contrast, our water temperature models used a 3-day averaged value of AOT instead of a single daily value. Yet a 3-day averaged value of smoke may still have been too short of a period for the larger watersheds we analyzed (e.g., main stem Klamath River locations) and will not fully capture effects from multiple consecutive days of smoke coverage, which is likely when the strongest effects occur. For example, in late July 2008, after a month of extensive smoke distribution over Northern California, water temperatures at many of the monitoring locations were the lowest observed for those calendar days across their entire respective time series. However, the cooling effect of smoke did not appear to be fully captured by the water temperature models during this period of time (Figure 6), possibly because water temperatures observed on these days were influenced by the persistent smoke coverage. For these reasons, we suspect that our modeled effects of wildfire smoke on water temperatures are likely underestimates of the true effects.

An alternative to our statistical regression approach would be to use an energy budget model to simulate the underlying physics of heat flux between a stream and its environment. Two recent models of Klamath and Trinity river water temperatures used this approach (Jones et al., 2016; Perry et al., 2011). While these models did not consider potential effects of wildfire smoke, the models did incorporate daily solar radiation and air temperature as primary drivers of water temperatures, suggesting that this modeling framework could be adapted to further elucidate the effects of smoke on lotic water temperatures.

5.5. Historical Context and Management Implications

Despite sources of uncertainty, these results suggest that wildfire smoke can cool lotic water temperatures in an ecologically meaningful way. In the Klamath-Siskiyou Mountains (Skinner et al., 2006; Taylor & Skinner, 1998, 2003), other regions of California (Stephens et al., 2007; Taylor et al., 2016), and much of the western USA (Marlon et al., 2012), wildfires occurred more frequently and annual area burned was greater prior to the onset of modern fire suppression in the early 20th century. This elevated wildfire activity would have resulted in extensive smoke production and frequently smoky skies during the summer and fall (Stephens et al., 2007). Thus, in watersheds where wildfires frequently occur under natural conditions, wildfire smoke can be a natural mechanism to reduce maximum river and stream water temperatures, conceivably benefiting cold-water adapted species such as Pacific salmon, char (*Salvelinus* spp.), and amphibians (e.g., Pacific giant salamander, *Dicamptodon tenebrosus*). Furthermore, because forest fire activity is often positively associated with air temperature and drought (Marlon et al., 2012; Taylor et al., 2016), significant smoke production is most likely to occur during years and seasons when water temperatures are highest and most stressful to cold-water adapted species.

In the lower Klamath River Basin, summer water temperatures often reach levels that are harmful to salmon and other cold-water adapted species (Bartholow, 2005; KRBFTF, 1991; NAS, 2004; NCRWQCB, 2010). Under these circumstances, even modest reductions of water temperatures by 1–2 °C due to wildfire smoke could have benefits to imperiled aquatic species. For example, adult Chinook salmon in the Klamath River exploit reductions in water temperatures resulting from reduced solar radiation and air temperature associated with weather fronts to migrate upstream (Strange, 2010). Both adult and juvenile salmon could similarly exploit smoke-induced cooling to migrate. Juvenile salmon also use localized thermal refuges within the lower Klamath Basin to avoid high water temperatures (e.g., Brewitt & Danner, 2014; Sutton & Soto, 2012). Smoke-induced cooling could produce spatially and temporally dynamic thermal refuges that increase the duration of time and areal extent of the river network that is useable for juvenile salmon during summer. Conversely, wildfire smoke may also affect lotic ecosystems in ways that could mitigate benefits of

reduced water temperatures. For instance, deposition of smoke and ash in streams can result in dramatic increases in nutrient concentrations and fluctuations of pH during and after wildfires, potentially harming aquatic organisms (Gresswell, 1999; Spencer et al., 2003).

While wildfire activity was greater in many watersheds of the western USA before the onset of modern fire suppression, fires generally burned at reduced intensities due to lower fuel loads (Steel et al., 2015). Lower fire intensities likely meant less smoke production per unit area burned than for fires in our analysis. It would be challenging to determine the net effect on water temperatures historically given a greater area burned but less smoke production per area burned. Even if less smoke was produced overall, more of the smoke may have remained in the river canyons historically because of fewer occurrences of smoke being injected far into the atmosphere by high intensity fires (e.g., Peterson et al., 2014; Val Martin et al., 2010), where it can be carried away by wind instead of remaining in the river canyons (see inversion discussion).

5.6. Conclusions

Wildfire smoke has well-documented negative effects on human health (Mott et al., 2002; Reid et al., 2016). These negative effects are often the only aspect considered in management of wildfire smoke, but there are opportunities for public health and ecological objectives to be aligned (Long et al., 2018). Here we evaluated an unappreciated but potentially important way in which wildfire smoke can influence lotic ecosystems. We hope our results contribute to a more holistic understanding of wildfire-aquatic ecosystem interactions to inform management of wildfires and wildfire smoke. Our results also add to recent research documenting diverse mechanisms through which wildfire can positively affect lotic ecosystem productivity (e.g., Boisramé et al., 2017; Flitcroft et al., 2016; Malison & Baxter, 2010). Together, these studies imply that in fire-prone ecosystems, the restoration of more natural fires regimes may help recover Pacific salmon populations and other imperiled aquatic species. Indeed, it is possible that a focus on dramatic, high-intensity fires and implementation of studies in fire-suppressed ecosystems has resulted in a biased perception of wildfire-aquatic ecosystem interactions. Ultimately, more research is needed on the ways that wildfire can shape lotic ecosystems. For example, we need to improve our understanding of the integrative thermal effects of wildfire smoke, the heat of combustion, and the loss of riparian vegetation on water temperature regimes in fire-prone watersheds.

Acknowledgments

We thank the organizations and people who collected and shared the water temperature data used in our analysis, particularly LeRoy Cyr and Jon Grunbaum of the U.S. Forest Service. The Klamath Tribal Water Quality Consortium partially funded J.E. Asarian's participation in this project. Nicholas Som (FWS) provided statistical advice. Sylvia Gwozdz and Brianna Walsh (FWS) assisted with data compilation and prepared Figure 1. Susan Fricke (Karuk Tribe), Crystal Robinson (Quartz Valley Indian Reservation), Matt Hanington (Yurok Tribe), Michelle Krall (Cramer Fish Sciences), and three anonymous reviewers provided feedback on earlier drafts of the manuscript. Finally, we thank the tribal members, scientists, and other community members in the Klamath River Basin who shared their insights and observations with us about the effects of wildfire on aquatic ecosystems in the region. Data supporting this analysis are archived in the online repository figshare (https://doi.org/10.6084/m9.figshare.5996477). The findings and conclusions in this article are those of the authors and do not necessarily represent the views of the U.S. Fish and Wildlife Service.

References

Abatzoglou, J. T. (2013). Development of gridded surface meteorological data for ecological applications and modelling. *International Journal of Climatology*, *33*(1), 121–131. https://doi.org/10.1002/joc.3413

Armstrong, J. B., Schindler, D. E., Omori, K. L., Ruff, C. P., & Quinn, T. P. (2010). Thermal heterogeneity mediates the effects of pulsed subsidies across a landscape. *Ecology*, *91*(5), 1445–1454. https://doi.org/10.1890/09-0790.1

Bartholow, J. M. (2005). Recent water temperature trends in the lower Klamath River, California. *North American Journal of Fisheries Management*, *25*(1), 152–162. https://doi.org/10.1577/M04-007.1

Beakes, M. P., Moore, J. W., Hayes, S. A., & Sogard, S. M. (2014). Wildfire and the effects of shifting stream temperature on salmonids. *Ecosphere*, *5*(5), art63. https://doi.org/10.1890/ES13-00325.1

Beitinger, T. L., & Fitzpatrick, L. C. (1979). Physiological and ecological correlates of preferred temperature in fish. *American Zoologist*, *19*(1), 319–329. https://doi.org/10.1093/icb/19.1.319

Benyahya, L., Caissie, D., St-Hilaire, A., Ouarda, T. B., & Bobée, B. (2007). A review of statistical water temperature models. *Canadian Water Resources Journal*, *32*(3), 179–192. https://doi.org/10.4296/cwrj3203179

Beschta, R. L., Bilby, R. E., Brown, G. W., Holtby, L. B., & Hofstra, T. D. (1987). Stream temperature and aquatic habitat: Fisheries and forestry interactions. In E. O. Salo & T. W. Cundy (Eds.), *Streamside management: Forestry and fishery interactions* (pp. 191–232). Seattle, WA: Institute of Forest Resources, University of Washington.

Blodgett, D. L., Booth, N. L., Kunicki, T. C., Walker, J. I., & Viger, R. J. (2011). Description and testing of the Geo Data Portal: Data integration framework and web processing services for environmental science collaboration (Open-File Report 2011–1157). U.S. Geological Survey.

Boisramé, G., Thompson, S., Collins, B., & Stephens, S. (2017). Managed wildfire effects on forest resilience and water in the Sierra Nevada. *Ecosystems*, *20*(4), 717–732. https://doi.org/10.1007/s10021-016-0048-1

Brenning, A. (2008). Statistical geocomputing combining R and SAGA: The example of landslide susceptibility analysis with generalized additive models. In J. Böhner, T. Blaschke, & L. Montanarella (Eds.), *SAGA—Seconds out* (pp. 23–32). Hamburg, Germany: Hamburger Beiträge zur Physischen Geographie und Landschaftsökologie.

Brewitt, K. S., & Danner, E. M. (2014). Spatio-temporal temperature variation influences juvenile steelhead (Oncorhynchus mykiss) use of thermal refuges. *Ecosphere*, *5*(7), art92. https://doi.org/10.1890/ES14-00036.1

Caissie, D. (2006). The thermal regime of rivers: A review. *Freshwater Biology*, *51*(8), 1389–1406. https://doi.org/10.1111/j.1365-2427.2006.01597.x

CARB (California Air Resources Board) (2013). Almanac emission projection data, 2012 estimated annual average emissions, Siskiyou County. California Environmental Protection Agency. Retrieved from https://www.arb.ca.gov/app/emsinv/2013/emssumcat_query.php?F_YR=2012&F_DIV=0&F_SEASON=A&SP=2013&F_AREA=DIS&F_DIS=SIS#9

Conrad, O. (2010). SAGA module close gaps with spline. SAGA—System for automated geoscientific analyses. Retrieved from http://www.saga-gis.org

Conrad, O., Bechtel, B., Bock, M., Dietrich, H., Fischer, E., Gerlitz, L., et al. (2015). System for automated geoscientific analyses (SAGA) v. 2.1.4. *Geoscientific Model Development*, *8*(7), 1991–2007. https://doi.org/10.5194/gmd-8-1991-2015

Core Team, R. (2015). *R: A language and environment for statistical computing*. Vienna, Austria: R Foundation for Statistical Computing. Retrieved from https://www.r-project.org/

Daly, C., Halbleib, M., Smith, J. I., Gibson, W. P., Doggett, M. K., Taylor, G. H., et al. (2008). Physiographically sensitive mapping of climatological temperature and precipitation across the conterminous United States. *International Journal of Climatology*, *28*(15), 2031–2064. https://doi.org/10.1002/joc.1688

Di, Q., Kloog, I., Koutrakis, P., Lyapustin, A., Wang, Y., & Schwartz, J. (2016). Assessing PM2.5 exposures with high spatiotemporal resolution across the continental United States. *Environmental Science & Technology*, *50*(9), 4712–4721. https://doi.org/10.1021/acs.est.5b06121

Dunham, J., Chandler, G., Rieman, B., & Martin, D. (2005). Measuring stream temperature with digital data loggers: A user's guide (RMRSGTR-150WWW) U.S. Department of Agriculture, Forest Service, Rocky Mountain Research Station.

Dunham, J., Lockwood, J., & Mebane, C. (2001). Issue paper 2: Salmonid distributions and temperature (EPA-910-D-01-002). Prepared as part of EPA region 10 temperature water quality criteria guidance development project.

Dunham, J. B., Rosenberger, A. E., Luce, C. H., & Rieman, B. E. (2007). Influences of wildfire and channel reorganization on spatial and temporal variation in stream temperature and the distribution of fish and amphibians. *Ecosystems*, *10*(2), 335–346. https://doi.org/10.1007/s10021-007-9029-8

Estes, B. L., Knapp, E. E., Skinner, C. N., Miller, J. D., & Preisler, H. K. (2017). Factors influencing fire severity under moderate burning conditions in the Klamath Mountains, northern California, USA. *Ecosphere*, *8*(5), arte01794. https://doi.org/10.1002/ecs2.1794

Flitcroft, R. L., Falke, J. A., Reeves, G. H., Hessburg, P. F., McNyset, K. M., & Benda, L. E. (2016). Wildfire may increase habitat quality for spring Chinook salmon in the Wenatchee River subbasin, WA, USA. *Forest Ecology and Management*, *359*, 126–140. https://doi.org/10.1016/j.foreco.2015.09.049

Gräler, B., Pebesma, E., & Heuvelink, G. (2016). Spatio-temporal interpolation using Gstat. *The R Journal*, *8*(1), 204–218.

Gresswell, R. E. (1999). Fire and aquatic ecosystems in forested biomes of North America. *Transactions of the American Fisheries Society*, *128*(2), 193–221. https://doi.org/10.1577/1548-8659(1999)128<0193:FAAEIF>2.0.CO;2

Hitt, N. P. (2003). Immediate effects of wildfire on stream temperature. *Journal of Freshwater Ecology*, *18*(1), 171–173. https://doi.org/10.1080/02705060.2003.9663964

Isaak, D. J., Luce, C. H., Rieman, B. E., Nagel, D. E., Peterson, E. E., Horan, D. L., et al. (2010). Effects of climate change and recent wildfires on stream temperature and thermal habitat for two salmonids in a mountain river network. *Ecological Applications*, *20*(5), 1350–1371. https://doi.org/10.1890/09-0822.1

Johnson, S. L. (2004). Factors influencing stream temperatures in small streams: Substrate effects and a shading experiment. *Canadian Journal of Fisheries and Aquatic Sciences*, *61*(6), 913–923. https://doi.org/10.1139/f04-040

Jones, E. C., Perry, R. W., Risley, J. C., Som, N. A., & Hetrick, N. J. (2016). Construction, calibration, and validation of the RBM10 water temperature model for the Trinity River, northern California. U.S. Geological Survey Open-File Report 2016–1056. https://doi.org/10.3133/ofr20161056

Keleher, C. J., & Rahel, F. J. (1996). Thermal limits to salmonid distributions in the Rocky Mountain region and potential habitat loss due to global warming: A geographic information system (GIS) approach. *Transactions of the American Fisheries Society*, *125*(1), 1–13. https://doi.org/10.1577/1548-8659(1996)125<0001:TLTSDI>2.3.CO;2

Klamath River Basin Fisheries Task Force (KRBFTF) (1991). Long range plan for the Klamath River Basin conservation area fishery restoration program.

Lake, F. K. (2007). Traditional ecological knowledge to develop and maintain fire regimes in Northwestern California, Klamath-Siskiyou Bioregion: Management and restoration of culturally significant habitats (doctoral dissertation). Corvallis, OR: Oregon State University.

Lake, F. K. (2013). Trails, fires, and tribulations: Tribal resource management and research issues in northern California. *Occasion: Interdisciplinary Studies in the Humanities*, *5*, 1–22.

Long, J. W., Tarnay, L. W., & North, M. P. (2018). Aligning smoke management with ecological and public health goals. *Journal of Forestry*, *116*(1), 76–86. https://doi.org/10.5849/jof.16-042

Lyapustin, A., Korkin, S., Wang, Y., Quayle, B., & Laszlo, I. (2012). Discrimination of biomass burning smoke and clouds in MAIAC algorithm. *Atmospheric Chemistry and Physics*, *12*(20), 9679–9686. https://doi.org/10.5194/acp-12-9679-2012

Lyapustin, A., Martonchik, J. V., Wang, Y., Laszlo, I., & Korkin, S. (2011). Multiangle implementation of atmospheric correction (MAIAC): 1. Radiative transfer basis and lookup tables. *Journal of Geophysical Research*, *116*, D03210. https://doi.org/10.1029/2010JD014985

Lyapustin, A., Wang, Y., Korkin, S., & Huang, D. (2018). MODIS collection 6 MAIAC algorithm. *Atmospheric Measurement Techniques Discussions*, 1–50. https://doi.org/10.5194/amt-2018-141

Lyapustin, A., Wang, Y., Laszlo, I., Kahn, R., Korkin, S., Remer, L., et al. (2011). Multiangle implementation of atmospheric correction (MAIAC): 2. Aerosol algorithm. *Journal of Geophysical Research*, *116*, D03211. https://doi.org/10.1029/2010JD014986

Lyapustin, A., Wang, Y., Laszlo, I., & Korkin, S. (2012). Improved cloud and snow screening in MAIAC aerosol retrievals using spectral and spatial analysis. *Atmosphere Measurement Techniques*, *5*(4), 843–850. https://doi.org/10.5194/amt-5-843-2012

Lyapustin, A. I., Wang, Y., Laszlo, I., Hilker, T., Hall, F. G., Sellers, P. J., et al. (2012). Multi-angle implementation of atmospheric correction for MODIS (MAIAC): 3. Atmospheric correction. *Remote Sensing of Environment*, *127*, 385–393. https://doi.org/10.1016/j.rse.2012.09.002

Mahlum, S. K., Eby, L. A., Young, M. K., Clancy, C. G., & Jakober, M. (2011). Effects of wildfire on stream temperatures in the Bitterroot River Basin, Montana. *International Journal of Wildland Fire*, *20*(2), 240–247. https://doi.org/10.1071/WF09132

Malison, R. L., & Baxter, C. V. (2010). The fire pulse: Wildfire stimulates flux of aquatic prey to terrestrial habitats driving increases in riparian consumers. *Canadian Journal of Fishery and Aquatic Sciences*, *67*(3), 570–579. https://doi.org/10.1139/F10-006

Marlon, J. R., Bartlein, P. J., Gavin, D. G., Long, C. J., Anderson, R. S., Briles, C. E., et al. (2012). Long-term perspective on wildfires in the western USA. *Proceedings of the National Academy of Sciences*, *109*(9), E535–E543. https://doi.org/10.1073/pnas.1112839109

McCullough, D. A. (1999). A review and synthesis of effects of alterations to the water temperature regime on freshwater life stages of salmonids, with special reference to Chinook salmon (EPA 910-R-99-010). Prepared for the U.S. Environmental Protection Agency region 10.

Miller, J. D., Skinner, C. N., Safford, H. D., Knapp, E. E., & Ramirez, C. M. (2012). Trends and causes of severity, size, and number of fires in northwestern California, USA. *Ecological Applications*, *22*(1), 184–203. https://doi.org/10.1890/10-2108.1

Minshall, G. W., Brock, J. T., & Varley, J. D. (1989). Wildfires and Yellowstone's stream ecosystems. *Bioscience*, *39*(10), 707–715. https://doi.org/10.2307/1311002

Mitášová, H., & Mitáš, L. (1993). Interpolation by regularized spline with tension: I. Theory and implementation. *Mathematical Geology*, *25*(6), 641–655. https://doi.org/10.1007/BF00893171

Mitchell, K. E., Lohmann, D., Houser, P. R., Wood, E. F., Schaake, J. C., Robock, A., et al. (2004). The multi-institution North American Land Data Assimilation System (NLDAS): Utilizing multiple GCIP products and partners in a continental distributed hydrological modeling system. *Journal of Geophysical Research*, *109*, D07S90. https://doi.org/10.1029/2003JD003823

Mott, J. A., Meyer, P., Mannino, D., Redd, S. C., Smith, E. M., Gotway-Crawford, C., & Chase, E. (2002). Wildland forest fire smoke: Health effects and intervention evaluation, Hoopa, California, 1999. *Western Journal of Medicine*, *176*(3), 157–162. https://doi.org/10.1136/ewjm.176.3.157

NAS (National Academy of Sciences) (1996). Upstream: Salmon and society in the Pacific Northwest. Committee on Protection and Management of Pacific Northwest Anadromous Salmonids.

NAS (National Academy of Sciences) (2004). Endangered and threatened fishes in the Klamath River Basin: Causes of decline and strategies for recovery. Committee on Endangered and Threatened Fishes in the Klamath River Basin.

NCRWQCB (North Coast Regional Water Quality Control Board) (2010). Final staff report for the Klamath River total maximum daily loads (TMDLs) addressing temperature, dissolved oxygen, nutrient, and microcystin impairments in California. Santa Rosa, CA.

Oyler, J. W., Ballantyne, A., Jencso, K., Sweet, M., & Running, S. W. (2015). Creating a topoclimatic daily air temperature dataset for the conterminous United States using homogenized station data and remotely sensed land skin temperature. *International Journal of Climatology*, *35*(9), 2258–2279. https://doi.org/10.1002/joc.4127

Perry, R. W., Risley, J. C., Brewer, S. J., Jones, E. C., & Rondorf, D. W. (2011). Simulating daily water temperatures of the Klamath River under dam removal and climate change scenarios. U.S. Geological Survey Open-File Report 2011–1243.

Peterson, D., Hyer, E., & Wang, J. (2014). Quantifying the potential for high-altitude smoke injection in the North American boreal forest using the standard MODIS fire products and subpixel-based methods. *Journal of Geophysical Research: Atmospheres*, *119*, 3401–3419. https://doi.org/10.1002/2013JD021067

Pinheiro, J., Bates, D., DebRoy, S., Sarkar, D., & Core Team, R. (2017). nlme: Linear and nonlinear mixed effects models. *R package version*, *3*, 1–131.

Poole, G. C., & Berman, C. H. (2001). An ecological perspective on in-stream temperature: Natural heat dynamics and mechanisms of human-caused thermal degradation. *Environmental Management*, *27*(6), 787–802. https://doi.org/10.1007/s002670010188

Reid, C. E., Brauer, M., Johnston, F. H., Jerrett, M., Balmes, J. R., & Elliott, C. T. (2016). Critical review of health impacts of wildfire smoke exposure. *Environmental Health Perspectives*, *124*(9), 1334–1343. https://doi.org/10.1289/ehp.1409277

Reid, C. E., Jerrett, M., Petersen, M. L., Pfister, G. G., Morefield, P. E., Tager, I. B., et al. (2015). Spatiotemporal prediction of fine particulate matter during the 2008 Northern California wildfires using machine learning. *Environmental Science & Technology*, *49*(6), 3887–3896. https://doi.org/10.1021/es505846r

Rieman, B. E., Gresswell, R. E., & Rinne, J. N. (2012). Fire and fish: A synthesis of observation and experience. In C. Luce, P. Morgan, K. Dwire, D. Isaak, Z. Holden, & B. Rieman (Eds.), *Climate change, forests, fire, water, and fish: Building resilient landscapes, streams, and managers* (pp. 159–175). Fort Collins, CO: U.S. Department of Agriculture, Forest Service.

Robinson, C. (2013). 2013 water quality study including impacts from fire: Salmon River, CA. Karuk Tribe Department of Natural Resources.

Robock, A. (1988). Enhancement of surface cooling due to forest fire smoke. *Science*, *242*(4880), 911–913. https://doi.org/10.1126/science.242.4880.911

Robock, A. (1991). Surface cooling due to forest fire smoke. *Journal of Geophysical Research*, *96*(D11), 20,869–20,878. https://doi.org/10.1029/91JD02043

Short, K. C. (2014). A spatial database of wildfires in the United States, 1992–2011. *Earth System Science Data*, *6*(1), 1–27. https://doi.org/10.5194/essd-6-1-2014

Short, K. C. (2017). *Spatial wildfire occurrence data for the United States, 1992–2015 [FPA_FOD_20170508]*, (4th ed.). Fort Collins, CO: Forest Service Research Data Archive. https://doi.org/10.2737/RDS-2013-0009.4

Shuter, B. J., & Post, J. R. (1990). Climate, population viability, and the zoogeography of temperate fishes. *Transactions of the American Fisheries Society*, *119*(2), 314–336. https://doi.org/10.1577/1548-8659(1990)119<0314:CPVATZ>2.3.CO;2

Skinner, C. N., Taylor, A. H., & Agee, J. K. (2006). Klamath Mountains bioregion. In N. G. Sugihara, J. W. van Wagtendonk, K. E. Shaffer, J. Fites-Kaufman, & A. E. Thode (Eds.), *Fire in California's ecosystems* (pp. 170–194). Berkeley, CA: University of California. https://doi.org/10.1525/california/9780520246058.003.0009

Spencer, C. N., Gabel, K. O., & Hauer, F. R. (2003). Wildfire effects on stream food webs and nutrient dynamics in Glacier National Park, USA. *Forest Ecology and Management*, *178*(1–2), 141–153. https://doi.org/10.1016/S0378-1127(03)00058-6

SRRC (Salmon River Restoration Council) (2014). Parched rivers & smoking skies: A year of drought and fire on the Salmon River. SRRC Fall/Winter 2014 Newsletter.

Steel, Z. L., Safford, H. D., & Viers, J. H. (2015). The fire frequency-severity relationship and the legacy of fire suppression in California forests. *Ecosphere*, *6*(1), art8. https://doi.org/10.1890/ES14-00224.1

Stephens, S. L., Martin, R. E., & Clinton, N. E. (2007). Prehistoric fire area and emissions from California's forests, woodlands, shrublands, and grasslands. *Forest Ecology and Management*, *251*(3), 205–216. https://doi.org/10.1016/j.foreco.2007.06.005

Stone, R. S., Augustine, J. A., Dutton, E. G., O'Neill, N. T., &, Saha A. (2011) Empirical determinations of the longwave and shortwave radiative forcing efficiencies of wildfire smoke. *Journal of Geophysical Research*, *116*, D12207. doi:https://doi.org/10.1029/2010JD015471

Strange, J. S. (2010). Upper thermal limits to migration in adult Chinook salmon: Evidence from the Klamath River Basin. *Transactions of the American Fisheries Society*, *139*(4), 1091–1108. https://doi.org/10.1577/T09-171.1

Superczynski, S. D., Kondragunta, S., & Lyapustin, A. I. (2017). Evaluation of the multi-angle implementation of atmospheric correction (MAIAC) aerosol algorithm through intercomparison with VIIRS aerosol products and AERONET: MAIAC AOT evaluation. *Journal of Geophysical Research: Atmospheres*, *122*, 3005–3022. https://doi.org/10.1002/2016JD025720

Sutton, R., & Soto, T. (2012). Juvenile coho salmon behavioral characteristics in Klamath River summer thermal refugia. *River Research and Applications*, *28*(3), 338–346. https://doi.org/10.1002/rra.1459

Taylor, A. H., & Skinner, C. N. (1998). Fire history and landscape dynamics in a late-successional reserve, Klamath Mountains, California, USA. *Forest Ecology and Management*, *111*(2–3), 285–301. https://doi.org/10.1016/S0378-1127(98)00342-9

Taylor, A. H., & Skinner, C. N. (2003). Spatial patterns and controls on historical fire regimes and forest structure in the Klamath Mountains. *Ecological Applications*, *13*(3), 704–719. https://doi.org/10.1890/1051-0761(2003)013[0704:SPACOH]2.0.CO;2

Taylor, A. H., Trouet, V., Skinner, C. N., & Stephens, S. (2016). Socioecological transitions trigger fire regime shifts and modulate fire-climate interactions in the Sierra Nevada, USA, 1600-2015 CE. *Proceedings of the National Academy of Sciences*, *113*(48), 13,684–13,689. https://doi.org/10.1073/pnas.1609775113

Val Martin, M., Logan, J. A., Kahn, R. A., Leung, F. -Y., Nelson, D. L., & Diner, D. J. (2010). Smoke injection heights from fires in North America: Analysis of 5 years of satellite observations. *Atmospheric Chemistry and Physics*, *10*(4), 1491–1510. https://doi.org/10.5194/acp-10-1491-2010

VanderKooi, S., Thorsteinson, L., & Clark, M. (2011). Environmental and historical setting. In L. Thorsteinson, S. VanderKooi, & W. Duffy (Eds.), *Proceedings of the Klamath Basin Science Conference, Medford, Oregon, February 1–5, 2010* (pp. 31–36). Reston, VA: U.S. Geological Survey.

Ward, J. V., & Stanford, J. A. (1982). Thermal responses in the evolutionary ecology of aquatic insects. *Annual Review of Entomology*, *27*(1), 97–117. https://doi.org/10.1146/annurev.en.27.010182.000525

Webb, B. W., Hannah, D. M., Moore, R. D., Brown, L. E., & Nobilis, F. (2008). Recent advances in stream and river temperature research. *Hydrological Processes*, *22*(7), 902–918. https://doi.org/10.1002/hyp.6994

Wiedinmyer, C., Akagi, S. K., Yokelson, R. J., Emmons, L. K., Al-Saadi, J. A., Orlando, J. J., & Soja, A. J. (2011). The Fire Inventory from NCAR (FINN): A high resolution global model to estimate the emissions from open burning. *Geoscientific Model Development*, *4*(3), 625–641. https://doi.org/10.5194/gmd-4-625-2011

Williams, J., & Curry, D. (2011). Watershed characterization. In L. Thorsteinson, S. VanderKooi, & W. Duffy (Eds.), *Proceedings of the Klamath Basin Science Conference, Medford, Oregon, February 1–5, 2010* (pp. 37–74). Reston, VA: U.S. Geological Survey.

Yu, P., Toon, O. B., Bardeen, C. G., Bucholtz, A., Rosenlof, K. H., Saide, P. E., et al. (2016). Surface dimming by the 2013 Rim Fire simulated by a sectional aerosol model. *Journal of Geophysical Research: Atmospheres*, *121*, 7079–7087. https://doi.org/10.1002/2015JD024702

Yvon-Durocher, G., Caffrey, J. M., Cescatti, A., Dossena, M., del Giorgio, P., Gasol, J. M., et al. (2012). Reconciling the temperature dependence of respiration across timescales and ecosystem types. *Nature*, *487*(7408), 472–476. https://doi.org/10.1038/nature11205

Zhang, J., Reid, J. S., Christensen, M., & Benedetti, A. (2016). An evaluation of the impact of aerosol particles on weather forecasts from a biomass burning aerosol event over the Midwestern United States: Observational-based analysis of surface temperature. *Atmospheric Chemistry and Physics*, *16*(10), 6475–6494. https://doi.org/10.5194/acp-16-6475-2016

Zuur, A. F., Ieno, E. N., Walker, N. J., Saveliev, A. A., & Smith, G. M. (2009). *Mixed effects models and extensions in ecology with R*. New York: Springer. https://doi.org/10.1007/978-0-387-87458-6